Rock Foundation, Yoshinaka & Kikuchi (eds) © 1995 Balkema, Rotterdam. ISBN 90 5410 562 3

# Stability and deformation analysis of complex rock foundations of several large dams and hydropower stations in China

Ge Xiurun, Feng Dingxiang, Gu Xianrong & Feng Shuren
*Institute of Rock and Soil Mechanics, Chinese Academy of Sciences, Wuhan, People's Republic of China*

ABSTRACT: On the basis of several examples of engineering projects of large dams and hydropower stations constructed on complex rock foundations, problems of sliding stability and deformation are analysed. A new method for safety factor against sliding is proposed. At the same time a new technique for evaluating initial geostresses through the in situ measured data of displacement is presented as well.

## 1 INTRODUCTION

The research on geoengineering problems in the construction of dams and hydropower stations is closely related with their rational design and safe operation. Projects of rock foundations in hydraulic structures involve a wide range of problems such as seepage, rock mass quality appraisal, reinforcement and improvement of rock mass. However, among them, stability and deformation are of great importance. As a rule, for the structure built on the rock foundation with weak intercalations, the problem of stability against sliding is of predominant significance, and forms a great concern for the designers. The serious interlayer dislocations and deformation in rock mass are discovered in a number of cases of power station projects in China when deep foundation pits are excavated in layered rock mass with weak intercalations. How to analyse the cause of this deformation, how to evaluate and predict the possible order of magnitude is also an important subject to be studied.

On the basis of several large dam and hydropower station projects in China, which have been completed or are under construction, we emphatically analyse the problem of stability and deformation, that is to say, the stability against sliding of dams built on the rock mass having weak intercalations, and the deformation of foundation pits in power stations. And the examples of analysis and calculation are also given. In this paper a "vectorial sum" method for safety factor against sliding is presented, which forms a new method due to its remarked difference from conventionally used methods. In this paper is also given a mechanical model and a calculation method for interlayer dislocations in the excavation in layered rock mass with weak intercalations. This method was used for the first time in the Gezhouba power station project, Yangtze River, China. The initial geostresses derived by means of this method are in good agreement with in situ measured data subsequently obtained. In recent years it found another successful application in Tianshengqiao hydropower project in China.

## 2 ANALYSIS OF STABILITY AGAINST SLIDING IN DEEP ROCK FOUNDATION AND APPRAISAL OF SLIDING RESISTANCE OF ROCK MASS

Here the in situ tests, numerical simulation and appraisal methods are given for the stability against sliding along the deep mudded intercalations and the sliding resistance of rock mass behind the dam in the Second Channel Sluice, Gezhouba project, Yangtze River, China.

The site of the project is situated on the lower mouth of the Three Gorges. It has the largest installed capacity among the hydropower stations in China. The Second Channel Sluice is the main discharge structure, which contains a 27-bay spillway. The sluicegate chamber has a dimension of $65\times18.5\times40m^3$. The largest hydrolic head is 27m. The water thrust acting on the gate is 1000 tones per meter. The rock foundation is formed by clayey siltstone. The rock layers lie nearly in horizontal direction with a very small dip angle of 4-8°. Among rock layers there are many mudded interculations. The depth of the main intercalation is about 10m below the chamber floor. The shear strength on the layer surfaces is low, therefore the stability against sliding along deep mudded intercalations becomes one of the main problems for this project. How to estimate the initial sliding resistance of rock mass behind the dam constitutes the key for solving this problem.

The physico-mechanical parameters for the bed rock and the mudded intercalations are obtained from in situ and laboratory tests. The deformation modulus for the clayey siltstone is 10-16 GPa, the wet compression strength is 8-10MPa; the shear strength is $\varphi=26.5°, c=0.05$MPa; the shear strength along the intercalations is $\varphi=24.2°, c=0.03$MPa.

### 2.1 Rigid body limit equilibrium analysis with consideration of resistance of rock mass behind the dam

According to the design standard, two sliding safety factors can be adopted:

$$K=\frac{f\Sigma W}{\Sigma p} \quad ; \quad K'=\frac{f'\Sigma W+c'A}{\Sigma P}$$

where $\Sigma W$ is the total normal force; $\Sigma P$ is the total tangential force, f shear friction coefficient; f' friction coefficient against shear failure, c' cohesion, A the section area of the dam foundation. In the above expressions no account is taken of the sliding resistance of the downstream rock foundation. Because of the considerable depth of the intercalations in the project, the rational results can be obtained only by modification of the above methods and consideration of this portion of sliding

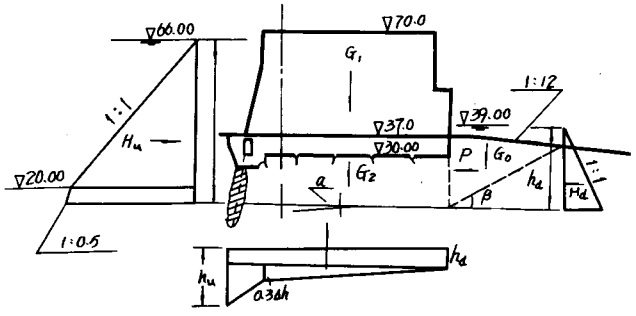


Figure 1. Loading.

resistance in the limit equilibrium analysis. Otherwise, the safety factor would become smaller at larger deptn of intercalations, which is apparently irrational.

## 2. 2 Formula for safety factor against sliding

Fig 1 gives a presentation for calculating loads. In consideration of sliding resistance of rock mass when the slide of rock mass downstream from the gate chamber takes place, the limit equilibrium formula is as follows:

$$K=\frac{f(\Sigma V\cos\alpha-\Sigma H\sin\alpha+P\sin\alpha)+P\cos\alpha}{\Sigma H\cos\alpha+\Sigma V\sin\alpha} \quad (1)$$

where f is friction coefficient, $\Sigma V$ is the vertical load above the intercalation, $\Sigma V = G_1 + G_2 - W$; $\Sigma H$ is the total horizontal load above the intercalation, P is the rock mass resistance; $\alpha$ is the dip angle of the intercalation. The sliding stability has a standard: $K \geqslant 1.30$.

## 2. 3 Evaluation of rock mass resistance P downstream from the chamber

The rationality of calculation of P strongly affects the results of stability analysis. Here it is assumed that the resistance P is in the horizontal direction and can be calculated through wedge limit equilibrium. According to geological conditions the most unfavorable fracture plane is taken as the first damage plane, and the related c and $\varphi$ is chosen. The downstream vertical plane in close vicinity of the gate is taken as the second damage plane. In order that a certain safety margin can be allowed in resistance calculation, the value of c for the first fracture plane is taken as zero, the resistance to shearing in the second fracture plane is negnected. Thus,

$$P=G_0 tg(\beta+\varphi) \quad (2)$$

where P is the rock mass resistance; Go the total vertical force on resistance block, $\beta$ the angle of the first fracture plane to the horizontal direction, $\varphi$ the friction angle of the first fracture plane ($\varphi=19.3°$).

## 2. 4 Large scale in situ tests for rock resistance

The resistant force o f the rock mass downstream from the chamber is essential for its sliding stability. For rationally evaluating the bearing capacity of the resistant rock mass behind the sluicegate, Yantze Valley Planning Office has carried out large scale in situ tests at the sites. There are 2 specimens. The specimen I has a dimension of $11.5\times1.7\times2.35m^3$, the specimen II has a size of $9.5\times1.7\times2.35m^3$. The uniform load acting on the top of specimen I is 0. 05MPa. No external load is applied on the specimen II.

Fig 2 indicates the specimen I. Fig 3 indicates the in situ stress-displacement curves of the two resistance blocks. The test damage strength of blocks I and II are 1. 53 and 1. 23MPa, respectively. The proportion limit is 0. 4—0. 5MPa, the yield strength 0. 8—0. 9MPa. In the limit equilibrium analysis the mean value of P is 0. 3—0. 36MPa, which is the third of the in situ yield value. Therefore the value of P used in the above analysis includes a margin and is on the safe side.

## 2. 5 Numerical simulation and elastic-brittle-plastic nonlinear analysis on the resistance block tests

The test process of resistance block I and II are simulated numerically. In Fig 4 is shown the meshing in the numerical simulation. The size is the same as that of in situ tests. The mechanical parameters are taken from the in situ tests. A main mudded surface called $202_4$(c=0. 005MPa, tg$\varphi$=0. 2) exists between the test block and the bed rock. There are also 3 horizontal layer surfaces with considerable shear strength: c = 0. 03MPa, tg$\varphi$ = 0. 88. Joint elements are used for simulating these weak surfaces, with the elasto-plastic properties and non-tension considered. The elastic-brittle-plastic model is adopted for rock elements (Fig 5a). The behaviour is elastic before the peak strength is reached. The stress drop occurs when the peak value is passed. The characteristics of brittle damage are simulated by stress transmission. When stresses fall to the residual srrength, they are simulated by means of elasto-plastic properties. When shear damage, that is to say, the brittle damage takes place and stresses drop abruptly, the first invariant of stress tensor for the element concerned is assumed constant. This means that volumetric deformation keeps unchanged at the stress drop. The original stress circle is reduced to a concentric circle tangential to the residual strength envelope (Fig 5b). Through evaluating the difference of these two circles can be obtained the values of released stresses, which then are conversed into related nodal forces and readjustment is performed. The abovementioned is the basic idea we use in treatment of the brittle properties.

Fig 6 gives the relation between the horizontal thrust and the area of damage zones of specimens I and II, which are obtained by the numerical simulation. It can be

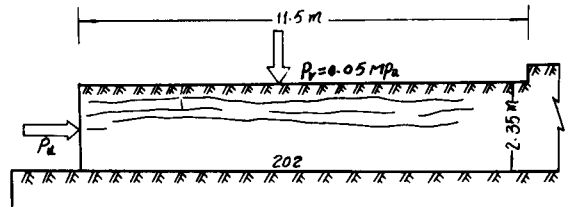


Figure 2. Resistant block test.

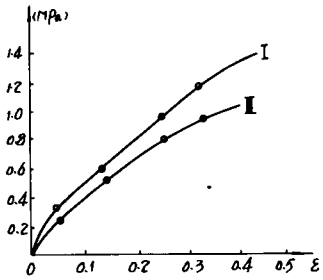


Figure 3. Stress-strain curves of resistant block.

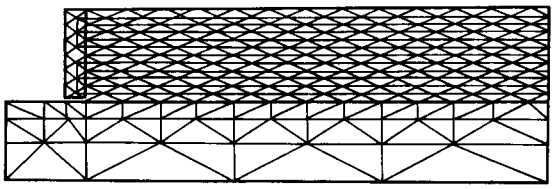

Figure 4. Meshing of resistant block.

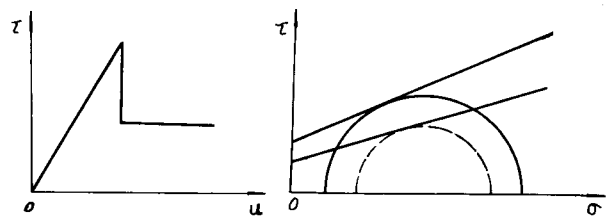


Figure 5. (a)τ~u curve. (b)τ~σ relation.

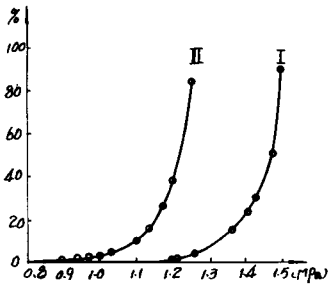


Figure 6. Curve of damage area VS. horizontal thrust.

seen that there is a good agreement. Test block Ⅱ taken as an example, the damage develops accelerately (Fig 6) when the horizontal trust reaches 1.1 MPa. This basically agrees with the characteric thrust P=1.064MPa recorded in situ, when the serious damage occurs.

Table 1 gives the comparison of test data of the main mudded surface and the whole resistance block to the related calculation results. Obviously, they are in good agreement.

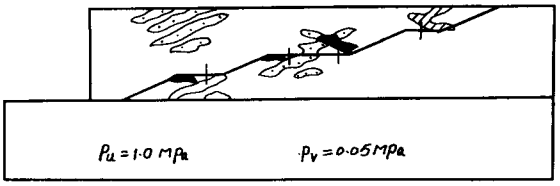


Figure 7. Damage of the resistant block with inclined fractures.

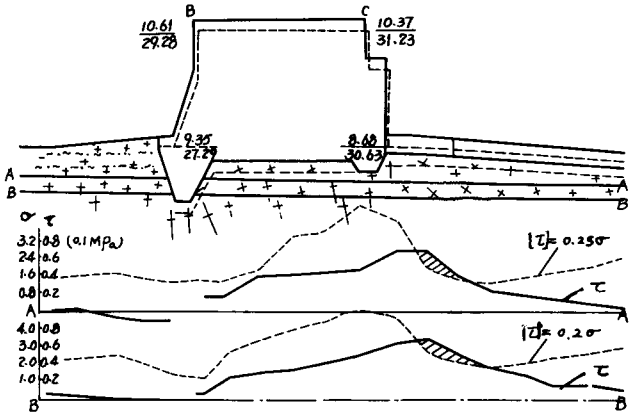


Figure 8. FEM results for the deep cutoff wall.

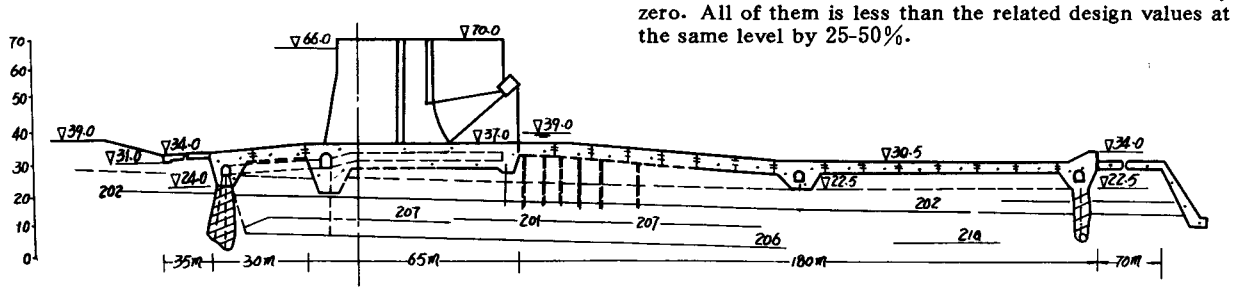


Figure 9. Treatment of sluicegate foundation.

Table 1. Comparison of test data to calculation results.

| Resistance block | | Ⅰ | Ⅱ |
|---|---|---|---|
| Vertical load (MPa) | | 0.05 | 0 |
| P (MPa) at the begining of the damage of main mudded surface | in situ test | 0.208 | 0.0532 |
| | calculation | 0.1 | 0.067 |
| P (MPa) when $202_4$ becomes a complete fracture surface | in situ test | 0.406 | 0.399 |
| | calculation | 0.5 | 0.4 |
| P (MPa) when damage of blocks takes place | in situ test | 1.534 | 1.24 |
| | calculation | 1.48 | 1.26 |

When the horizontal thrust on a unit area reached 0.467MPa a sliding surface of zigzag shape composed of inclined fracture surfaces and layer surfaces is formed. When the thrust rises to 0.567MPa, the opening of the sliding surface occurs. The damage of rock blocks begins at 0.7MPa of the thrust. The damage zones in the resistance block containing zigzag fracture planes at 1.1MPa of the horizontal thrust per a unit area is shown in Fig 7.

It is obvious that the value of P used in limit equilibrium is far below the capacity of the rock mass behind the gate even if declined joint surfaces exist.

### 2.6 FEM analysis on stability against sliding in the large depth in the Second Channel Sluice

The elastic-brittle-plastic non-linear analysis is the same as the above-mentioned. The plane problem is considered. Numerous schemes of reinforcement such as deep cutoff walls, seepage prevention slabs have been calculated. The length of calculation range in the upstream direction is twice the floor length, while the range arrived downstream at the anti-scour wall. The depth of the range equals the floor length. For the sake of space only the FEM results of the scheme of the cutoff wall is given (Fig 8). The so-called deep cutoff wall is made of concrete at the front of the chamber and goes past the mudded intercalations. From the stress distribution in the mudded intercalations it can be seen that within the section of 20m which is behind the chamber the resistance of the mudded intercalation is less than the sliding force, therefore it is a yield section, though the safety factor is about 2.0. According to the FEM results the resistance force of the rock mass behind the chamber is the third of the total resistance, therefore it is important in the analysis.

### 2.7 Foundation treatment

Because the resistant rock mass of the bays 1-6 in the Second Channel Sluice is weak and have inclined cracks, the safety degree for these bays is lower compared with others'. On the basis of the FEM results comprehensive measures of reinforcement and improvement including piles are taken, which are shown in Fig 9 (Xu et al., 1983). Observed data show that after the impoundment in the Gezhouba project the horizontal displacement of the gate chamber is 1-3mm, the vertical settlement 3-5mm, the relative dislocation of the mudded intercalation nearly zero. All of them is less than the related design values at the same level by 25-50%.

## 3 MODEL TEST AND NUMERICAL SIMULATION FOR SLIDING STABILITY OF A GRAVITY DAM

Through loading tests and numerical simulation on the model dam the study is to be made on the process of the damage, which takes place at the sliding plane composed of two weak intercalations in the deep portion of the foundation. The verification of the numerical analysis is also to be peformed (X. R. Gu et. al, 1987).

### 3.1 Model test on sliding stability of the gravity dam

The body and foundation of the model dam are made of gupsum. The height of the model dam is 0.6m, and thickness 0.1m. In the rock foundation there are 2 weak intercalations, which exert a predominant effect on sliding stability. The physico-mechanical parameters are given in Table 2.

Table 2. The physico-mechanical parameters.

| | E (MPa) | V | Compression strength (MPa) | tgφ | C (MPa) | γ ($10^3$N/m$^3$) |
|---|---|---|---|---|---|---|
| Rock | 1650 | 0.2 | 1.9 | 0.87 | 0.4 | 6 |
| weak inter. | 10 | 0.2 | | 0.317 | 0 | |

In the test, first of all, a vertical pressure of 4000N is applied to simulate self-weight. Then the horizontal loads are exerted in a step-wise way (Table 3) until failure takes place.

Table 3. Horizontal loading steps with standard thrust $P_0$=1323N.

| step | 1 | 2 | 3 | 4 | 5 | 6 | 7 | 8 | 9 |
|---|---|---|---|---|---|---|---|---|---|
| $p/p_0$ | 0.25 | 0.5 | 0.75 | 1.0 | 1.25 | 1.5 | 1.75 | 2.0 | 2.25 |

The test indicates that slide begins at the overload of 1.25 and the final loss of stability takes place at the overload of 2.25.

### 3.2 Numerical simulation of the model dam test

The non-linear behaviours of joints which are used for simulation of weak intercalation of model dam foundation are shown in Fig 10.

The mesh of deformation corresponding to the 9th loading step ($P/P_0$=2.25) is shown in Fig 11.

Relative displacement between the corresponding points on the top and bottom of weak intercalations are related to the increasing horizontal loading steps as shown in Fig 12 and Fig 13. Fig 13 indicates that sliding plane A opens gradually with loading increasing. As for plane B, the situation is complicated; opeing of the edge section increases as load increases, while the other section remains in compaction.

### 3.3 Progressive failure of sliding surface in rock foundation

The progressive failure of sliding surface is shown in Fig 14. It coincides very well with the model testing data, indicating the complete loss of sliding stability of model dam foundation at P=2.25$P_0$.

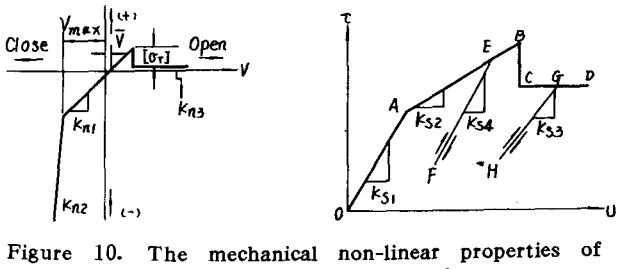


Figure 10. The mechanical non-linear properties of weakplanes (a) Normal Deformation model; (b) Shear displacement model;

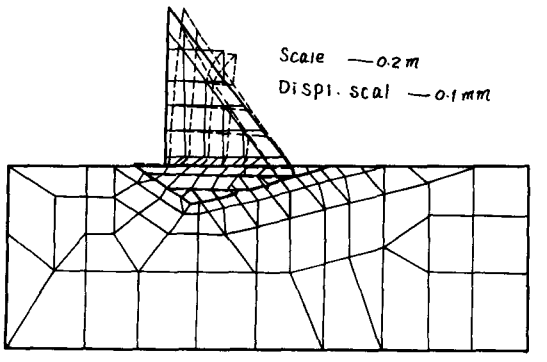


Figure 11. Mesh deformation of the model dam.

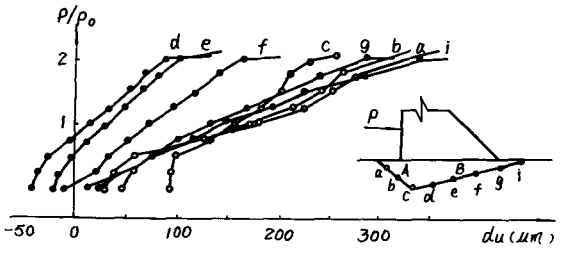


Figure 12. Tangential displacement of intercalation.

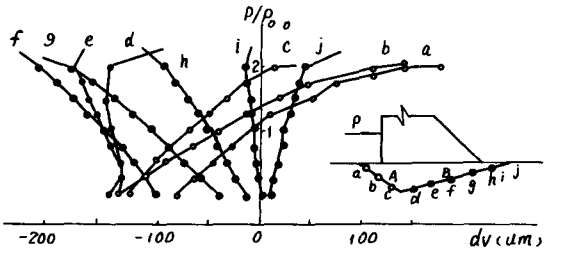


Figure 13. Normal displacement of intercalation.

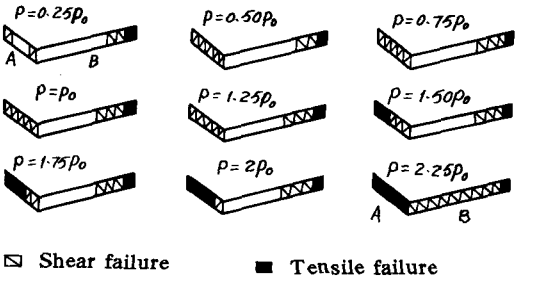


Figure 14. Progressive failure process.

## 4 A NEW METHOD OF CALCULATING THE SAFETY FACTOR FOR STABILITY AGAINST SLIDING

### 4.1 Conventional method based on the principle of "algebraic sum"

When the distribution of the normal and tangential stresses σ and τ on the potential sliding surfuce are obtained in some way, say, in FEM analysis, it is needed to evaluate the safety factor against sliding. Usually the following formula is adopted:

$$K=\frac{\sum_{i=1}^{n}(\sigma_i f_i \Delta L_i + C_i \Delta L_i)}{\sum_{i=1}^{n}\tau_i \Delta L_i} \quad (3)$$

where

$\sigma_i, \tau_i$ normal and tangential stress of element i on the sliding plane;

$f_i, c_i$ friction coefficient and cohesion for material of element i;

$\Delta L_i$ length of element i along sliding plane;

n total number of elements on sliding plane.

However, the conception of the formula based on the principle of "algebraic sum" seems to be questionable.

As is well known, only if the potential sliding surface is a portion of circular arc, then the numerator of the expression can be regarded as the sum of moments of resistance forces with respect to the center of the arc, and the denominator as the sum of moments of sliding forces with respect to the same center. With the radius eliminated in the expression by reduction, the numerator and the denominator become the algebraic sums of resistance forces and sliding forces on the sections of the potential sliding surface. It is apparent that the expression (3) has clear-cut physical meaning only when the sliding surface is a circular arc, or nearly a circular arc, or a straight line segment.

### 4.2 A new conception of calculating the safety factor for stability against sliding

The new conception presented by the first author of this paper is based on the basic of the following considerations.

1. It is known from the practice that in many occasions the potential sliding surfaces in the rock foundations and slopes can be simplified, as a rule, into multiple line segments.

2. The different sections on the potential sliding surface differ in their role. Each surface usually are divided into two basic portions: sliding-resistent portion and sliding portion.

3. All the forces acting on the potential sliding surface are vectors. It is right to make a comparison after the resistance and sliding forces are superposed respectively, but this superposition should be vectorical, i. e., the vectorial sum rather than the algebraic one is to be used.

4. This superposition should be made with respect to a base plane. It is logical to select the main resistane portion on the sliding surface as the base plane.

### 4.3 New method for calculating K on the basis of vectorial sum

The vectorial sum can finally lead to the following formula the derivation of which is omitted for the sake of space:

$$K=\frac{\sum_{i=1}^{n}\sigma_i \Delta L_i \sin\alpha_i + \sum_{i=1}^{n}\Delta\sigma_i \Delta L_i f_i \cos\alpha_i + \sum_{i=1}^{n} c_i \Delta L_i \cos\alpha_i}{\sum_{i=1}^{n}\sigma_i \Delta L_i \sin\alpha_i + \sum_{i=1}^{n}\tau_i \Delta L_i \cos\alpha_i} \quad (4)$$

where $\alpha_i$ is the angle of the main sliding-resistent plane selected to the sliding section i. When the potential sliding direction is in quadrant I or IV (Fig 15a) the $\alpha_i$ in clockwise sense is negative. When this direction is in quadrant II or III (Fig 15b) the $\alpha_i$ in counterclockwise sense is negative. The compressive $\sigma_i$ is positive, the sliding resistent $\tau_i$ is positive, as shown in Fig a, b.

### 4.4 Application I

The safety factor and the horizontal thrust are evaluated with the two methods, respectively, in the above-mentioned example of gravity dam. The relation curves are shown in Fig 16. Generally, the values of K obtained through the "vectorial sum" method are less than that through the "algebraic sum" method. But they tend to become identical at the limit state. Values of K from the "vectorial sum" have a nearly linear relation with the horizontal thrust. This may reflect the variation tendancy more realistically and makes it possible to obtain the maximal overload at K = 1 through calculation of several values of overload.

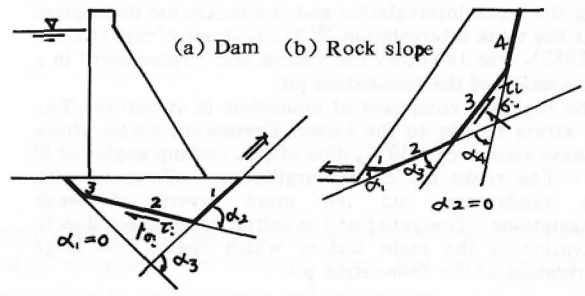


Figure 15. Potential sliding surface

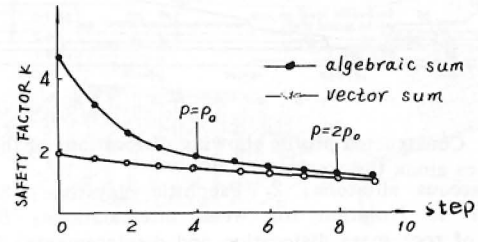


Figure 16. Safety factors against sliding.

### 4.5 Application II

Ankang dam is a gravity dam on the Han River, the largest tributary of Yangtze River. It has very complicated rock foundation which contain 5 fault belts and 6 weak intercalations. The distribution of principal stresses obtained from plane FEM non-linear analysis is shown in Fig 17.

The safety factors for selected types of possible glide tracks are listed in Table 4.

Table 4. Safety factors against sliding of Ankang Gravity Dam.

| Method | Composition of sliding planes | | |
|---|---|---|---|
| | $F_2-J_1-F_3$ | $F_2-J_1-F_4$ | $F_2-J_1-J_2$ |
| Conventional method (Algebraic sum) | 3.26 | 2.45 | 1.99 |
| New Method (Vector sum) | 2.00 | 1.85 | 1.70 |

It can be found that the dam is in a stable operation condition under normal loads. The discontinuity set of $F_2-J_1-J_2$ forms the dangerest potentical sliding planes for the dam rock foundation.

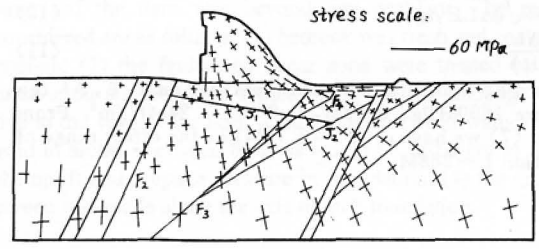


Figure 17. Principal stress distribution.

## 5 DISPLACEMENT ANALYSIS OF THE ROCK FOUNDATION PIT FOR THE GEZHOUBA HYDROPOWER PLANT №2

After the foundation pit of the Gezhouba hydropower plant №2 was excavated to its initial configuration remakable horizontal dislocations of the residual wall of presplit holes and the large bore holes were discovered along the weak intercalation and the maximum dislocation along the weak intercalation № 212 is about 80mm (Ge et. al. 1982). Fig 18 shows the sliding and displacement in a cross section of the foundation pit.

The region is composed of monocline in structure. The rock strata belong to the Lower Cretaceous series strata and have strikes of N30°E, dips of SE, and dip angles of 6° — 8°. The rocks are chiefly argillaceous siltstones with little sandstones and ten more layers of weak intercalations. The relief of the initial geostresses due to excavation is the main factors which caused the large deformation of the foundation pit.

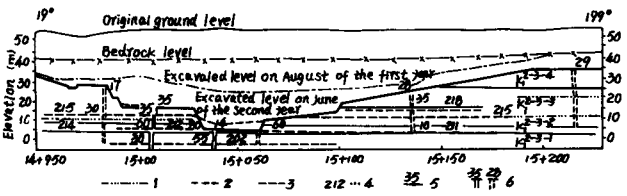


Figure 18. Constructed profile showing dislocations of the rock masses along the weak intercalations
1. Argillaccous siltstone; 2. Psephitic claystone; 3. Claystone; 4. Notation for weak intercalations; 5. Dircction of rock-mass dislocation and displacements; in mm; 6. Notation for C 1000mm bore boles.

### 5.1 The method for estimating the initial geostress based on the displacements of foundation pit observed in situ

First, on the basis of characteristics of horizontal layered rock mass a mechanical model is established for theoretical analysis, as shown in Fig 19a. The distribution of the longitudinal strain ε is given in Fig 19b.

According to the model we have

$$\int_0^H \sigma_x(y)dy=\int_0^L \tau(x)dx \tag{5}$$

where L and H are the length and depth of stress disturbance zone respectively.

Assume that

$$\varepsilon(x)=\varepsilon_{max}\left(\frac{x}{L}\right)^2 \tag{6}$$

$$\tau(x)=\tau_{max}\left[1-\left(\frac{L-x}{L}\right)^2\right] \tag{7}$$

and ΔL indicates the sliding distance of rock mass along the weak intercalation. Then we have

$$\Delta L=\int_0^L \varepsilon(x)dx=\frac{2}{3}\varepsilon_{max}\cdot L \tag{8}$$

$$\varepsilon_{max}=\frac{\bar{\sigma}_x(y)}{E}=\frac{1}{E}\frac{\int_0^H \sigma_x(y)dy}{H} \tag{9}$$

If $\sigma_x(y)$ distributes linearly and the cohesion C is negnected, then

$$\sigma_x(H)=\sqrt{8\Delta L E\gamma tg\varphi} \tag{10}$$

$$L=\frac{6E\Delta L}{\sigma_x(H)} \tag{11}$$

According to in situ tests and measured data, E, ΔL tgφ and γ are 1660MPa, 0.08m, 0.3 and 0.24MN/m³. From (6) and (7) we have $\sigma_x(H)=2.77$MPa, the effect range of dislocation L=288M.

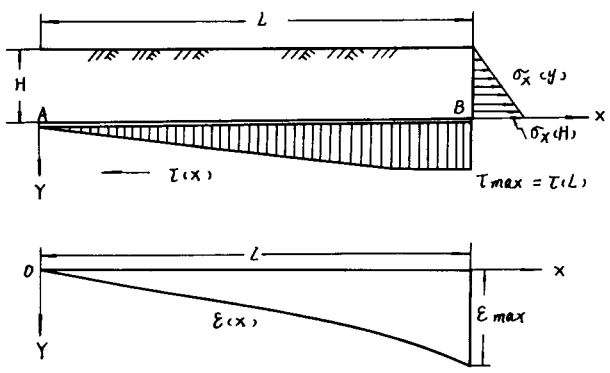


Figure 19. Distribution of ε(x).

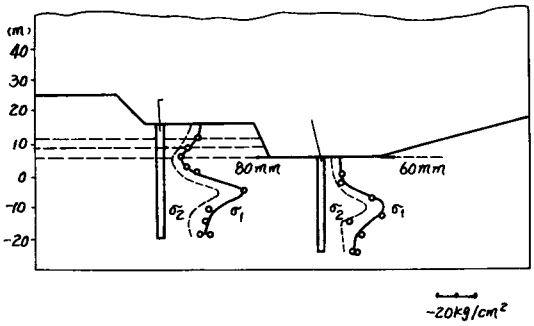


Figure 20. Distribution of geostresses $\sigma_1$ and $\sigma_2$.

### 5.2 The stress measurment in situ

In order to check and demostrate the direction and amount of the residual geostress of rock the stress measurement has been done in situ and three boreholes have been especially set up. By means of the overcoring technique for every borehole from the ground surface to the depth of 40m the stress measurement was carried out at 8 — 10 point. The data are shown in Fig 20.

The in situ measured data are $\sigma_1=-3.1$MPa and $\sigma_2=-2.3$MPa, which are in good agreement with the calculation value. In Tianshengqiao hydropower project the in situ measured data are $\sigma_1=13.9$MPa, $\sigma_2=9.8$MPa, $\sigma_3=1.6$MPa, while the calcuted $\sigma_1=14$MPa. These two examples indicate that the above analysis method has a universal significance.

## REFERENCES


Xu, L. X. et. al. 1983. Sliding stability of foundation rock with shear zones. Proceedings of 5th Int. Congress on Rock Mechanics. Melbourne, Vol. 1. p205—208.

Gu, X. R., Li, J. & Ge, X. R. 1987. Analysis of stability aganist sliding of a gravity dam by means of microcomputer. Proceedings of 2nd EPMESC, Guangzhou, Vol 3, p474—477.

Ge, X. R., Feng, D. X. & Yang, J. L., 1982. The elasto-visco-plastic analysis for rock displacement of the foundation pit of a water power plant. Rock Mechanics, Vol 15, p145—161.